INTEGRA

RICERCA & SVILUPPO

"A FIBRE ELEMENT FOR CYCLIC BENDING AND SHEAR. I: THEORY"

Petrangeli, M., Pinto, P.E. and Ciampi, V. (1999)

"Questo articolo è stato pubblicato per la prima volta sulla rivista *Journal of Engineering Mechanics*, casa editrice: ASCE, http://www.asce.org/"

"This article was first published in *Journal of Engineering Mechanics*, publisher: ASCE, http://www.asce.org/"

"Cet article a été publié pour la première fois sur *Journal of Engineering Mechanics*, éditions: ASCE, http://www.asce.org/"

"Este artículo se publicó por primera vez en la revista *Journal of Engineering Mechanics*, casa editorial : ASCE, http://www.asce.org/"

FIBER ELEMENT FOR CYCLIC BENDING AND SHEAR OF RC STRUCTURES. I: THEORY

By Marco Petrangeli,[1] Paolo Emilio Pinto,[2] and Vincenzo Ciampi[3]

ABSTRACT: After a few years of successful application of the fiber beam element to the analysis of reinforced concrete (RC) frames, the introduction of the mechanisms of shear deformation and strength appears to be the next necessary step toward a realistic description of the ultimate behavior of shear sensitive structures. This paper presents a new finite-beam element for modeling the shear behavior and its interaction with the axial force and the bending moment in RC beams and columns. This new element, based on the fiber section discretization, shares many features with the traditional fiber beam element to which it reduces, as a limit case, when the shear forces are negligible. The element basic concept is to model the shear mechanism at each concrete fiber of the cross sections, assuming the strain field of the section as given by the superposition of the classical plane section hypothesis for the longitudinal strain field with an assigned distribution over the cross section for the shear strain field. Transverse strains are instead determined by imposing the equilibrium between the concrete and the transverse steel reinforcement. The nonlinear solution algorithm for the element uses an innovative equilibrium-based iterative procedure. The resulting model, although computationally more demanding than the traditional fiber element, has proved to be very efficient in the analysis of shear sensitive RC structures under cyclic loads where the full 2D and 3D models are often too onerous.

INTRODUCTION

When the shear span ratio is below 2, the behavior of elements loaded monotonically to failure becomes brittle, due either to diagonal crushing of concrete in the web region and/or to the opening of wide inclined cracks.

Under cyclic loads, the mechanics of these short elements are such that they cannot be made acceptably ductile and dissipative by simply increasing the amount of lateral reinforcement, unless the longitudinal reinforcement and the axial force are also within proper, narrow, ranges.

The shear problem, however, tends to dominate the high-cycle behavior for slender, essentially flexural, elements. It may be stated that ultimately all cyclic failures are shear failures, whether due to the desegregation of concrete within doubly diagonal cracks, or to the localized slip between the two faces of large flexural cracks.

The reduction of shear capacity due to cyclic loading in the ductility range, as a function of the axial force, is now recognized in recent United States codes (''Building'' 1995). The degraded shear strength must still be larger than the flexural strength if a premature shear failure is to be avoided.

The need for complete models that are capable of describing the full range of the behavior of elements under axial force, bending, and shear is particularly acute in earthquake engineering, where the design is purposely made for the limit state of collapse (''R.C.'' 1996a,b). Ideally, the analyses should be performed using realistically degrading and failing elements, to be able to monitor the response of the whole structure down to its final state. The lack of reliable elements of this type obscures our capability of judging whether a structure has failed or not, and it is among the major sources of error in the quantification of the design forces.

Today, the most promising numerical modeling of reinforced concrete (RC) elements is either carried out with 2D and 3D finite elements or by monodimensional fiber elements. The former are computationally very demanding and therefore are seldom if ever used in the cyclic or dynamic analysis of RC structures. At the present time these models are mainly exploited for the understanding of the failure mechanisms of concrete specimens under monotonic loading, providing a reference for the corresponding laboratory tests. The fiber models are capable of describing the flexural behavior and its interaction with the axial force in slender beam-column elements, and are therefore widely used in structural analysis applications, although they do not provide full insight on the failure mechanisms of these elements.

The proposed fiber model with shear capabilities is situated between the two approaches previously discussed. Its formulation is based on an innovative and effective iterative solution procedure for the nonlinear beam problem, presented in Petrangeli and Ciampi (1997). While substantially retaining the speed and handiness of the traditional fiber model, the new element is capable of accounting for the stress-strain field arising in a beam-column element due to combined axial, bending, and shear force. The model has full cyclic capabilities.

Part II of this paper (Petrangeli 1999) will calibrate and verify the fiber model by experimental data. An application to a well-known structural collapse that occurred during the 1995 Hyogoken Nambu earthquake will be also presented.

BASIC ASSUMPTIONS

The proposed new model is based on the fiber beam element developed by Petrangeli (1991, 1996). This element included various features from previous fiber elements (Powell 1982; Kaba and Mahin 1984; Mari 1984; Zeris and Mahin 1988), together with some original contributions that made it a robust and easy to use tool for the dynamic analysis of RC structures (Petrangeli and Pinto 1994). The principal ingredients of this classical fiber element that have been retained in the new model are as follows.

- Equilibrium-based integrals for the element solution.
- Fixed monitoring sections located at Gauss's points along the element.
- Fiber discretization for force and stiffness integration over the sections.
- Explicit algebraic constitutive relations for concrete and steel based on the state-of-the-art formulations.

[1]Asst. Prof., Facu. of Arch., Univ. ''G. D'Annunzio,'' 65127 Pescara, Italy.

[2]Prof. of Earthquake Engrg., Dept. of Struct. and Geotech. Engrg., Rome Univ. ''La Sapienza,'' Rome, Italy.

[3]Prof. of Struct. Mech., Dept. of Struct. and Geotech. Engrg., Rome Univ. ''La Sapienza,'' Rome, Italy.

Note. Associate Editor: Sunil Saigal. Discussion open until February 1, 2000. Separate discussions should be submitted for the individual papers in this symposium. To extend the closing date one month, a written request must be filed with the ASCE Manager of Journals. The manuscript for this paper was submitted for review and possible publication on January 7, 1998. This paper is part of the ***Journal of Engineering Mechanics***, Vol. 125, No. 9, September, 1999. ©ASCE, ISSN 0733-9399/99/0009-0994–1001/$8.00 + $.50 per page. Paper No. 17310.

The flow chart of the element solution procedure for the classical fiber element developed by the writers is shown in Fig. 1.

The new element, while incorporating the above features, differentiates from the previous element by having two additional strain fields to be monitored at each cross section, namely, the shear strain field and the lateral field. The shear strain field comes explicitly in the element formulation, the lateral field is statically condensed at each section by imposing the equilibrium between transverse steel and concrete. For a 2D beam, the section strain and stress field vectors therefore read

$$\mathbf{q}(\xi) = (\varepsilon_0 \phi \gamma) \tag{1}$$

$$\mathbf{p}(\xi) = (\mathcal{N} \mathcal{M} \mathcal{T}) \tag{2}$$

where ε_0 = axial strain; ϕ = section curvature; γ = shear deformation; and $\mathcal{N}$, $\mathcal{M}$, and $\mathcal{T}$ = axial force, bending moment, and shear force, respectively. These generalized strains and stresses are functions of the element normalized abscissa $\xi = x/l$.

Given the section strain vector $\mathbf{q}(\xi)$, the fiber longitudinal and shear strains are found using suitable section shape functions. In particular, for the longitudinal strain field (parallel to the beam axis), the plane section hypothesis has been retained, whereas for the shear strain field different shear shape functions can be used. Constant and parabolic shape functions have been tested, with equally acceptable results in both cases. The strain of the ith fiber found from the section kinematic variables $\mathbf{q}(\xi)$ and the above-mentioned hypotheses can therefore be written

$$\epsilon_x^i(\xi) = \varepsilon_0(\xi) - \phi(\xi) Y^i \tag{3}$$

$$\epsilon_{xy}^i(\xi) = \gamma(\xi) \quad \text{or} \quad \epsilon_{xy}^i(\xi) = \frac{3}{2}\gamma(\xi)\left[1 - \left(\frac{Y^i}{H/2}\right)^2\right] \tag{4}$$

where Y^i = distance of the ith fiber from the section centroid; and H = section height.

The use of a predefined shear strain function greatly enhances the element performance in terms of robustness and speed, although it is clearly a source of inaccuracy. In this context the work of Vecchio and Collins (1988) should be mentioned. These authors suggest finding the section shear strain profile from the equilibrium of two adjacent sections, and have compared this approach with that of using predefined section shear shape functions. Their findings seem to indicate that the use of a kinematic constraint is an approximation consistent with the overall approximation of the beam modeling.

The lateral strain field is found by imposing the equilibrium in the lateral direction. Because the fiber longitudinal and shear strain (ϵ_x^i, ϵ_{xy}^i) are found from (3) and (4), the strain in the transverse direction ϵ_y^i remains as the only unknown. By imposing the equilibrium in the lateral direction, a complete 2D strain tensor at each concrete fiber $\boldsymbol{\epsilon}^i = (\epsilon_x \epsilon_y \epsilon_{xy})$ is therefore found. A schematic representation of the fiber and section strain field is plotted in Fig. 2.

When imposing the equilibrium between concrete and steel in the transverse direction, we can choose any solution within two extreme options, which are, respectively: (1) Impose equilibrium at each fiber separately; and (2) impose equilibrium over the whole section. With Option 1 the equilibrium is imposed globally assuming $\sigma_y = \sigma_y^i$ as constant over the section (Bažant and Bath 1977). Under this assumption, the stirrups act as unbonded ties. In Option 1 instead, equilibrium is enforced at each fiber, assuming a perfect bond, and therefore, $\sigma_y^j \neq \sigma_y^i$. In between the two cases we could, in principle, choose to impose equilibrium separately over groups of fibers, based, for example, on the section geometry and stirrup configuration.

In case lateral equilibrium is imposed at each fiber separately (Option 1), the following equation must be satisfied:

$$\sigma_{y,c}^i A_{y,c}^i + \sigma_{y,s}^i A_{y,s}^i = 0, \quad i = 1, 2, \ldots, nc \tag{5}$$

where $\sigma_{y,c}^i = \sigma_{y,c}^i(\epsilon_x^i \epsilon_y^i \epsilon_{xy}^i)$ = concrete stress in the transverse direction at the ith fiber; $\sigma_{y,s}^i = \sigma(\epsilon_y^i)$ = stress in the stirrup at the same fiber; and $A_{y,c}^i$ and $A_{y,s}^i$ = their respective areas in Y (transverse) direction.

If lateral equilibrium is imposed over the whole section (Option 2), we have instead

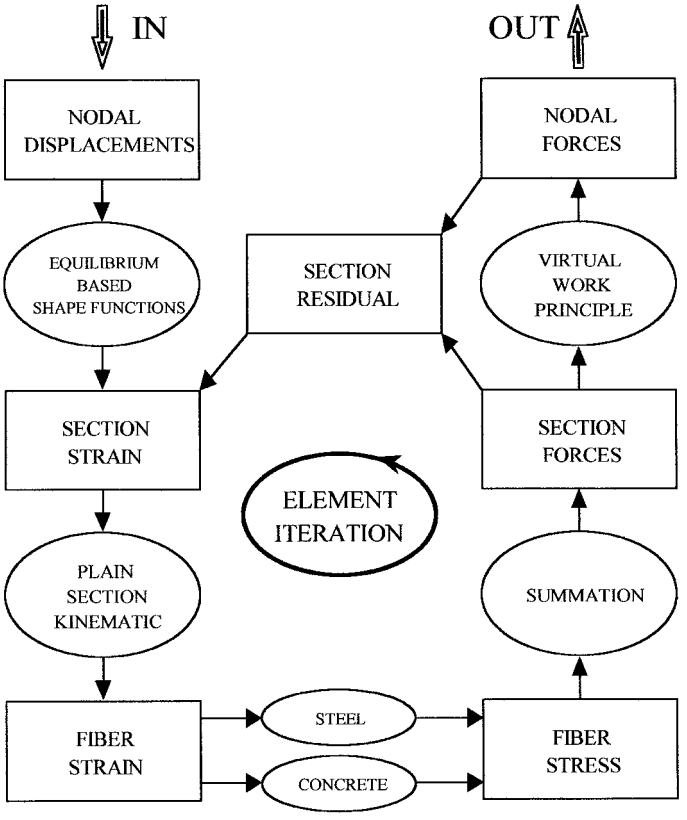

FIG. 1. Element State Determination for Flexural Fiber Model

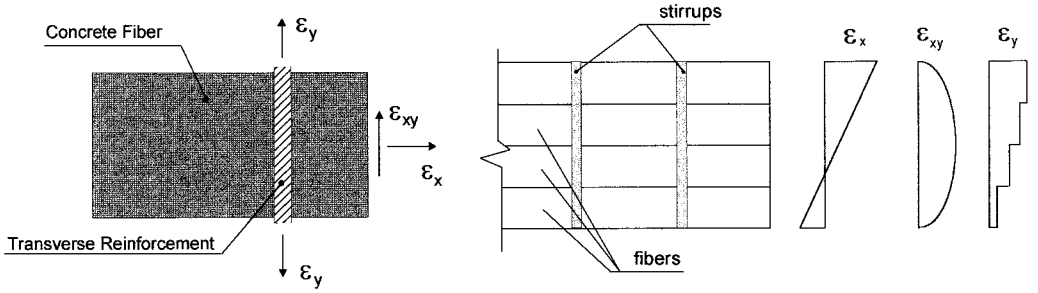

FIG. 2. Section and Fiber Mechanics

$$\sigma^i_{y,c} A^i_{y,c} + \sigma_{y,s} A_{y,s} = 0, \quad i = 1, 2, \ldots, nc \tag{6}$$

where $\sigma_{y,s} = \sigma(\bar{\epsilon}_{y,s})$ = a function of the average lateral strain $\bar{\epsilon}_{y,s}$ over the section given by the following expression:

$$\bar{\epsilon}_{y,s} = \frac{\sum_{i=1}^{nc} \epsilon^i_{y,c} A^i_{x,c}}{\sum_{i=1}^{nc} A^i_{x,c}} \tag{7}$$

where the strains have been averaged using the longitudinal concrete fiber area $A^i_{x,c}$.

Regarding the choice of Option 1 or 2, the following comments are relevant:

- Option 1 is generally more convenient as it provides a satisfactory approximation for sections of a general type, including thin wall or hollow sections where the assumption of constant transverse confining stresses σ_y would be unrealistic (Petrangeli et al. 1995). This approach gives the possibility of specifying a different ''effective'' transverse steel area for each fiber, depending on the stirrup configuration. For example, the concrete cover can be modeled without confinement, and inside the core different degrees of confinements can be specified for different fibers.
- Both approaches require as many lateral strain field unknowns as the number of concrete fibers. Imposing the equilibrium globally still requires a different lateral strain field in each concrete fiber (longitudinal and shear strains are generally not constant over the section), to satisfy equilibrium with the confining effect of steel. The difference between the two approaches is that with Option 2 there exists only one transverse steel fiber, compared with Option 1, where the transverse steel fibers are as numerous as the longitudinal concrete fibers subjected to its confinement action.
- Option 1 is more advantageous from a computational point of view because the iterations are carried out separately, at each fiber, according to the degree of nonlinearity of the fiber behavior. Therefore, the total number of fiber state determinations are reduced to a minimum, avoiding iteration of the whole section, as with Option 2, when highly nonlinear behavior takes place in only a few fibers. The iterations on local constitutive behavior (i.e., constitutive behavior monitoring) for these models represent the bulk of the computational demand and must therefore be accurately optimized.
- In the majority of RC members, externally applied lateral forces are zero [see (5) and (6)]. It would be easy, however, to consider an external state of stress in the lateral direction as in the case, for example, of external wrapping of columns.

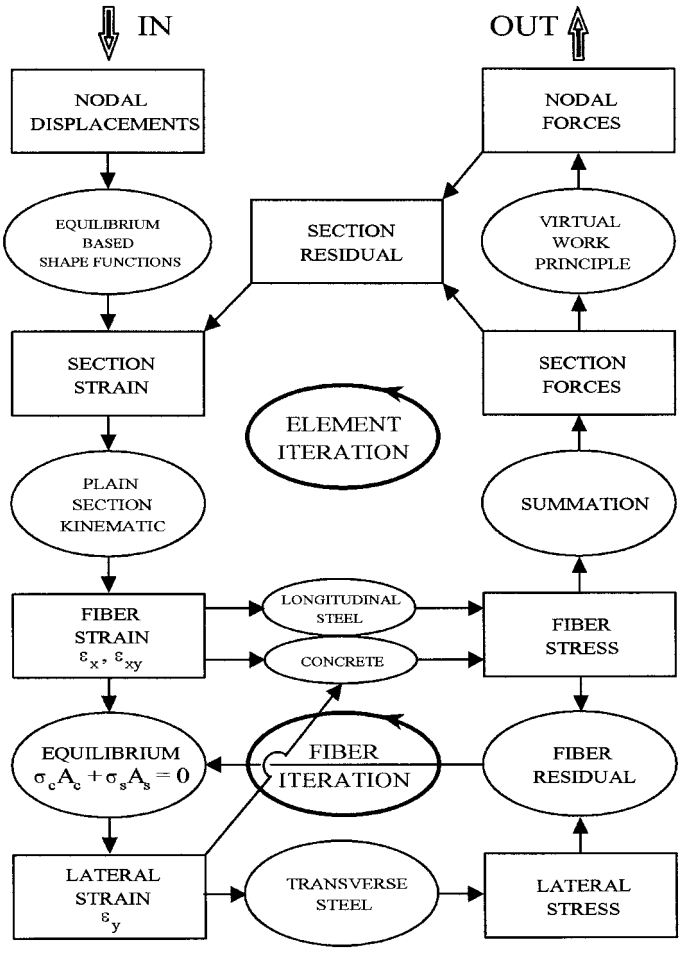

FIG. 3. Element State Determination for Shear Enhanced Fiber Model

The solution procedure (state determination) for the new fiber beam element is summarized in the flow chart of Fig. 3. Compared with the classical fiber element, the addition of a nested loop for the satisfaction of the lateral equilibrium is necessary. This loop requires the constitutive monitoring of the transverse steel fibers that are not assumed to be active in the flexural fiber model. The major difference with the classical model, however, lies in the necessity of using a constitutive low for concrete capable of describing, as accurately as feasible, the interaction between the longitudinal and the transverse response (2D or 3D type).

CONSTITUTIVE BEHAVIORS

Although a beam element does allow for some simplification in the material modeling with respect to a full 3D problem [e.g., there is no need to describe crack propagation that is so often the cause for mesh dependency and stress locking in 2D and 3D applications (Petrangeli and Ožbolt 1996)], still, the element response is entirely dependent on the concrete model capability to correctly predict the material response. Shear resisting mechanisms are completely governed by the concrete behavior and its interaction with transverse steel. Contrary to the so-called strut and tie or truss approaches, where only the compressive concrete strut needs to be modeled while the tensile part is carried by the steel ties (Garstka et al. 1993; Guedes and Pinto 1997; Ranzo and Petrangeli 1998), the proposed element is closer to a model of a RC continuum based on a reduced number of degrees of freedom following the beam schematization.

The search for a reliable and robust concrete constitutive model with cyclic capabilities has been therefore a major task in the element development. Satisfactory results were achieved with an equivalent uniaxial approach (Petrangeli et al. 1995), but a more consistent and robust solution has been obtained by exploiting the ''microplane'' approach (Bažant and Oh 1985; Bažant and Prat 1988; Bažant and Ožbolt 1990; Ožbolt and Bažant 1992).

As widely known, the microplane family of models is based on a kinematic constraint relating the external strains with those on selected internal planes, and on the monitoring of simple stress-strain relationships on these planes. The approach greatly enhances the cyclic capability and simplifies the numerical modeling of the softening behavior of concrete. The original model presents a few drawbacks, particularly when it attempts to model the different failure mechanisms in

tension and compression with the same set of parameters. A clarification of this problem is useful to better appreciate the reasons behind the proposed new constitutive model.

Quasi-brittle heterogeneous material such as concrete exhibits the following macroscopic behavior (e.g., in a laboratory specimen): Lateral deformations (expansion) at peak load in a uniaxial compression test are much larger than the principal elongation at peak load in a uniaxial tension test. Material models based on strain monitoring should therefore behave differently, whether they are in predominant tensile or compressive conditions. The use of invariants such as deviatoric, volumetric, or other strain indicators does not help in this respect.

The original microplane formulation instead did not modify the stress-strain relations for the microplane normal and shear components depending on the predominant stress state; these stress-strain laws were assumed to be independent from each other, the stresses on each microplane only depending on the assigned stress-strain law and the corresponding microplane strain. This leads to some inconsistent results. Suppose, for example, that the tensile branch of the microplane stress-strain laws is calibrated to match the behavior of a concrete specimen in a uniaxial tension test (Fig. 4). If the model, with the same setting, is subjected to uniaxial compression, the lateral expansion strain on the microplanes perpendicular to the applied compression reaches the maximum resistance well before peak load and goes into the softening branch. As a consequence, the model shows a strong dilatancy, which in real concrete only takes place around squash load. Vice versa, by calibrating the microplane tensile behavior to match the lateral response of concrete in compression, the model yields unrealistic strength in direct tension (Petrangeli et al. 1993). It can be easily verified that the use of deviatoric instead of normal components does exacerbate the problem because deviatoric strains are larger than normal ones in the direction perpendicular to the applied compression (i.e., $\epsilon_D = \epsilon_N - \epsilon_V > \epsilon_N$, when $\epsilon_V < 0$).

This difference between lateral toughness in compression and direct tension strength is peculiar to heterogeneous quasi-brittle materials and is handled by most of the available concrete constitutive models by coupling two different failure mechanisms.

Various modifications of the original microplane model have been proposed to overcome the above-said weaknesses (Bažant et al. 1996; Ožbolt 1996). In the present paper a new solution is proposed that can be described as a two-phase, kinematically constrained constitutive model based on the microplane approach. The model links together the microplane approach and an equivalent uniaxial rotating concept for the strain partitioning between the two material phases (components).

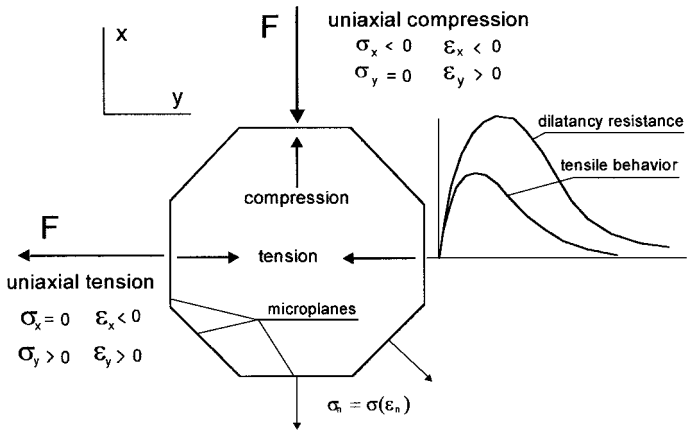

FIG. 4. Tensile Strength versus Lateral Dilatancy in Microplane Approach

The idea for the proposed model comes from the lateral stress distribution under uniaxial compression that takes place in heterogeneous materials made of components with different Young's modulus and Poisson's ratios, as, for example, masonry. In these cases the stiffer components tend to laterally confine the others, as the brick does with the mortar. Therefore, in a two-element schematization (aggregate/cement) under uniaxial compression, the lateral stresses are null only in an integral sense, with the stiffer aggregate being in tension and the cement paste in compression.

Finding the concrete fiber macrostress tensor associated with the corresponding strain $\boldsymbol{\sigma}^i = \boldsymbol{\sigma}(\boldsymbol{\epsilon}^i)$ requires the following step, with all expressions written for the 2D case.

Strains are partitioned into a ''weak'' $\boldsymbol{\epsilon}^w$ and a ''strong'' $\boldsymbol{\epsilon}^s$ component. Partitioning is carried out along the principal strain directions, similar to an equivalent uniaxial approach

$$\bar{\boldsymbol{\epsilon}}^s = \boldsymbol{\Phi}\bar{\boldsymbol{\epsilon}} \tag{8}$$

$$\bar{\boldsymbol{\epsilon}}^w = \bar{\boldsymbol{\epsilon}} - \bar{\boldsymbol{\epsilon}}^s \tag{9}$$

where the overlined tensors refer to the principal strain reference system and the matrix $\boldsymbol{\Phi}$ is given by the following expression:

$$\boldsymbol{\Phi} = \Phi_0 \phi(\epsilon^{dam}) \begin{bmatrix} 0 & -1 & 0 \\ -1 & 0 & 0 \\ 0 & 0 & 0 \end{bmatrix} \tag{10}$$

where $0 \leq \Phi_0 \leq \nu$ is a constant, with ν being the Poisson's ratio, whereas $\phi(\epsilon^{dam})$ provides an index of the residual cohesion in the material $[0 \leq \phi(\epsilon^{dam}) \leq 1]$ as a function of a strain-based damage indicator.

In the linear elastic regime, when $\phi = \phi(\epsilon^{dam}) = 1$, the splitting between the strong and weak component is governed by Φ_0. Setting $\Phi_0 = 0$ causes the strong component to vanish with all of the strains going into the weak one. Increasing Φ_0 up to the Poisson's coefficient reduces the amount of confining strain carried by the weak component under uniaxial compression. When $\Phi_0 = \nu$, the lateral strains in the weak component vanish and all of the confining stresses are provided by the strong component.

In the nonlinear regime instead, the splitting of the total strain tensor into the weak and strong components, starting from the assigned value of Φ_0, is governed by the evolution of the $\phi = \phi(\epsilon^{dam})$ function. A simple exponential expression has been used so far with satisfactory results. No cycling rules are required because the function works as a damage index that retains the maximum value during unloading and reloading branches. Further refinement could be investigated, introducing an energy dependency in addition to the maximum strain. The following expression performed the best in the numerical implementation:

$$\phi(\epsilon^{dam}) = e^{(\epsilon^{dam}/e_0)^p}, \quad \epsilon^{dam} = \epsilon^D \epsilon_2^{\max} \tag{11}$$

where ϵ^D = deviatoric invariant; $\epsilon_2^{\max}$ = maximum compressive strain; and e_0 and p = constants.

Once the two macrostrain components have been found, the model follows the microplane approach where the macrostrain tensors are projected onto planes evenly distributed around the circumference to obtain the microplane weak e^w and strong e^s normal strain components

$$e_k^w = \mathbf{A}_k \boldsymbol{\epsilon}^w; \quad e_k^s = \mathbf{A}_k \boldsymbol{\epsilon}^s \tag{12a,b}$$

where $\mathbf{A}_k$ = standard transformation matrix between the k-microplane orientation and the first principal strain or, alternatively, between the former and the beam reference system, in which case the macrostrain tensors [(8) and (9)] are first trans-

formed back into the beam reference system and then projected onto the microplanes. With only microplane normal components to be monitored, the $\mathbf{A}_k$ matrix is made of a single row; calling θ_k the angle between the two reference systems, it has the usual form

$$\mathbf{A}_k = [\cos^2\theta_k \ \sin^2\theta_k \ \sin\theta_k \cos\theta_k] \tag{13}$$

The stresses in the material are then found, for the two components, using the microplane constitutive behaviors

$$s_k^w = s(e_k^w); \quad s_k^s = C_k^s e_k^s \tag{14a,b}$$

where the constitutive model for the weak element is a nonlinear algebraic expression with a set of rules for the loading and unloading branches, whereas the strong element is assumed to be linear elastic. The mathematical expression used for the weak component will be described in the companion paper, and although based on an accurate formulation by Mander et al. (1988), it could be replaced with other expressions without making any conceptual difference to the model.

It should be noticed that the weak and strong components are not in series, in the sense that $s_k^w \neq s_k^s$, and are not in parallel, in the sense that $e_k^w \neq e_k^s$. The following relations apply between the k-microplane stress σ_k and strain ϵ_k, and the corresponding weak and strong components:

$$\epsilon_k = e_k^w + e_k^s; \quad \sigma_k = s_k^w + s_k^s \tag{15a,b}$$

The macrostress tensor $\boldsymbol{\sigma} = (\sigma_x \sigma_y \sigma_{xy})$ is finally obtained by integrating the microplane normal stress components over the unit circumference using the virtual work principle

$$\pi \, d\boldsymbol{\sigma}^T \delta\boldsymbol{\epsilon} = \int_{\mathcal{C}} d\sigma_k \delta\epsilon_k \, d\mathcal{C} = \int_{\mathcal{C}} (ds_k^w + ds_k^s)(\delta e_k^w + \delta e_k^s) \, d\mathcal{C} \tag{16}$$

substituting (8) and (9) into (12), and again into (16), we obtain

$$d\boldsymbol{\sigma} = \frac{2}{\pi} \int_0^\pi \mathbf{A}_k^T (ds_k^w + ds_k^s) \, d\theta \tag{17}$$

The integral is carried out over half-circumference because of the stress tensor symmetry. The concrete fiber constitutive matrix $\mathbf{D}$ can be similarly found using an incremental form of the microplane constitutive behaviors (14)

$$ds_k^s = C_k^w \, de_k^w; \quad ds_k^s = C_k^s \, de_k^s \tag{18a,b}$$

where C_k^w = tangent modulus of the microplane weak stress-strain relationship. Substituting (8) and (9) into (12), and again into (18), (17) can be rearranged as follows:

$$d\boldsymbol{\sigma} = \mathbf{D} \, d\boldsymbol{\epsilon} = \frac{2}{\pi} \left[\int_0^\pi \mathbf{A}_k^T C_k^w \mathbf{A}_k \, d\theta + \boldsymbol{\Phi}^T \int_0^\pi \mathbf{A}_k^T (C_k^s - C_k^w) \mathbf{A}_k \, d\theta \right] d\boldsymbol{\epsilon} \tag{19}$$

The integrals in (17) and (19) are to be numerically evaluated by monitoring a number of microplanes distributed over the circumference. The greatest efficiency is achieved with a regular (uniform) distribution of an even number of integration points to profit from the strain tensor symmetry by monitoring only half of them. In the numerical implementation of the proposed model, the eight-point discretization has been mainly used, although the response it provides is not invariant to the strain loading direction. This sensitivity, particularly in the softening regime, has been analyzed in detail by comparing different integration formulas for the 3D case (surface of a sphere) by Bažant and Oh (1985).

For the beam case, the model sensitivity to the principal strain orientation with respect to the microplane orientation is not particularly significant. The microplanes orientation is determined by the beam axis, and therefore, as long as the material response is consistent, the lack of directional invariance, appreciable only in the softening regime, can be disregarded.

In the linear elastic regime, assuming isotropy of the microplane material constraints, the following relations are found:

$$D_{11} = D_{22} = \frac{C^w}{4}(3 + \Phi_0) - \frac{C^s}{4}\Phi_0 \tag{20a}$$

$$D_{12} = D_{21} = \frac{C^w}{4}(1 + 3\Phi_0) - \frac{C^s}{4}3\Phi_0 \tag{20b}$$

$$D_{33} = \frac{C^w}{4}(1 + \Phi_0) - \frac{C^s}{4}\Phi_0 \tag{20c}$$

where the other terms are null. The identification of the above elements of the stiffness matrix terms with the well-known constants for isotropic elastic materials in plane stress conditions yields the following relations between C^w, C^s, Φ_0, and Young's modulus and Poisson's ratio E, ν of concrete:

$$C^w = \frac{E}{1-\nu^2}\frac{3-\nu}{2}; \quad C^s = \frac{E}{1-\nu^2}\frac{1-3\nu+3\Phi_0-\nu\Phi_0}{2\Phi_0} \tag{21a,b}$$

Although the proposed splitting of the microplane strains into weak and strong components bears only a qualitative resemblance to the physical mechanisms taking place in concrete materials, it has shown to be very useful because it depicts the obvious fact that the strains tend to localize in the weak components such the cement paste and the interface while unloading takes place in the strong elements such as the aggregates. The proposed approach also provides a consistent solution for the compression toughness of concrete materials having a very limited tensile strength.

As for the steel, both longitudinal and transversal, a monodimensional nonlinear constitutive relation, detailed in the companion paper, is used and does not need further comments at this stage.

SECTION FORCES AND STIFFNESS

Once the section deformations [(1)] are known following the element solution strategy discussed in the next paragraph, the corresponding forces [(2)] and stiffnesses must be found using the section kinematic [(3) and (4)] and the fiber constitutive behaviors.

Because the fiber transverse strains are unknown, the nonlinear equation [(5) and (6)] must be solved iteratively. The fiber stiffness matrices used in these iterations, as well as the ones needed at the element level, must account for the effect of the confining steel. This is done by way of a static condensation of the degree of freedom in the transverse Y-direction. Calling α^i the following transverse reinforcement ratio:

$$\alpha^i = \frac{A_{y,c}^i}{E_{y,s}^i A_{y,s}^i + D_{22}^i A_{y,c}^i} \tag{22}$$

where $A_{y,c}^i$ = area of ith concrete fiber in the transverse direction; and $A_{y,s}^i$, $E_{y,s}^i$ = area and the tangent modulus of the tributary transverse steel, the fiber axial and shear stiffness are found as follows:

$$K_a^i = (D_{11}^i - D_{12}^i D_{21}^i \alpha^i) \tag{23}$$

$$K_s^i = (D_{33}^i - D_{23}^i D_{32}^i \alpha^i) \tag{24}$$

the out-of-diagonal terms, null in the linear elastic range, are

$$K_{as}^i = (D_{13}^i - D_{12}^i D_{23}^i \alpha^i) \tag{25}$$

$$K_{sa}^i = (D_{31}^i - D_{32}^i D_{21}^i \alpha^i) \tag{26}$$

The concrete fiber incremental constitutive relation, taking into account the transverse steel contribution, can therefore be written

$$\begin{bmatrix} d\sigma^i_{x,c} \\ d\sigma^i_{xy,c} \end{bmatrix} = \begin{bmatrix} K^i_a & K^i_{as} \\ K^i_{sa} & K^i_s \end{bmatrix} \begin{bmatrix} d\epsilon^i_{x,c} \\ d\epsilon^i_{xy,c} \end{bmatrix} \tag{27}$$

A similar and simpler incremental relationship can be stated for the longitudinal steel using its monodimensional nonlinear constitutive relation.

Once all of the fibers' incremental constitutive behaviors are known, the section forces are found by way of the summation, of the concrete fiber longitudinal and shear stress increments $\Delta\sigma^i_{x,c}$ and $\Delta\sigma^i_{xy,c}$, and of the longitudinal steel fiber stress increments $\Delta\sigma^j_{x,s}$. The resulting axial $\Delta\mathcal{N}$, bending $\Delta\mathcal{M}$, and shear force $\Delta\mathcal{T}$ increments are found as follows:

$$\Delta\mathcal{N} = \sum_{i=1}^{nc} \Delta\sigma^i_{x,c} A^i_{x,c} + \sum_{j=1}^{ns} \Delta\sigma^j_{x,s} A^j_{x,s} \tag{28a}$$

$$\Delta\mathcal{M} = \sum_{i=1}^{nc} \Delta\sigma^i_{x,c} A^i_{x,c} Y^i_c + \sum_{j=1}^{ns} \Delta\sigma^j_{x,s} A^j_{x,s} Y^j_s \tag{28b}$$

$$\Delta\mathcal{T} = \sum_{i=1}^{nc} \Delta\sigma^i_{xy,c} A^i_{x,c} \tag{28c}$$

where $A^i_{x,c}$ and $A^j_{x,s}$ = areas of the ith concrete fiber and the jth steel fiber in the longitudinal direction (parallel to the beam axis); and Y^i_c, Y^j_s = their distances from the section centroid. From (28), the section incremental constitutive relation can be derived in the form

$$\Delta\mathbf{p}(\xi) = \mathbf{k}(\xi)\Delta\mathbf{q}(\xi) + \mathbf{r}_p(\xi) \tag{29}$$

where $\mathbf{r}_p(\xi)$ = section force residuals; and $\mathbf{k}(\xi)$ = section stiffness matrix found by substituting (3) and (4) into the fiber incremental constitutive equations and again into (28).

The element algorithm is such [see (36) in the next paragraph], that (29) is not explicitly used because there is no need for an explicit estimate of the section residuals. The section subroutine only needs to find, at each iteration step, the section forces associated to assigned section deformations $\mathbf{p}(\xi) = \mathbf{p}[\mathbf{q}(\xi)]$; a task that becomes particularly straightforward when explicit algebraic expressions $\sigma = \sigma(\epsilon)$ are used for the fiber constitutive behaviors.

In the proposed section behavior, the direct contribution of the longitudinal steel to the shear force and stiffness has been omitted, although for large deformation the so-called ''dowel action'' may not be negligible. This mechanism is currently being added into the model by way of a modification of the longitudinal steel subroutine, where other phenomena such as rebar buckling can be accounted for as well.

ITERATIVE ALGORITHM AT ELEMENT LEVEL

The solution method, used at the element level for integrating the section forces and deformations to obtain the corresponding nodal values, plays a very important role in the element architecture. The peculiarity of the beam element, whose equilibrium integrals are known, can be used to obtain element algorithms that are far more efficient than the traditional stiffness approach, and from that the derived assumed strain field methods (Simo and Rifai 1990).

An efficient element solution can save time threefold: (1) By increasing the element accuracy; (2) by reducing the number of sections to be monitored along the element; and (3) by requiring fewer element iterations to converge. These advantages have been obtained with the equilibrium-based iterative solutions briefly discussed in the following. These methods stem out of the traditional flexibility approach when the latter

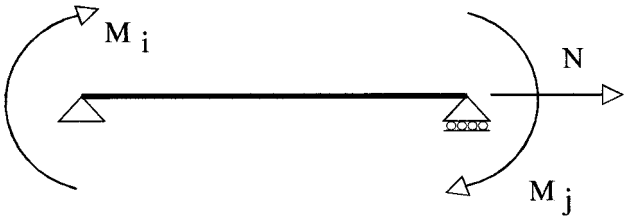

FIG. 5. Element Nodal Forces

are to be implemented in a beam element with assigned node displacements, as shown in Petrangeli and Ciampi (1997). A simpler derivation of this algorithm, for a finite-beam element to be implemented in a standard finite-element program, can be obtained as follows.

From nodal element displacements, section strains need to be found. This task, which in the standard stiffness approach is accomplished using predefined element shape functions, is now performed in an iterative fashion. An initial solution is found using the following expression:

$$\Delta\mathbf{q}(\xi)_0 = \mathbf{a}(\xi)\Delta\mathbf{Q} = \mathbf{f}_0(\xi)\mathbf{b}(\xi)\mathbf{F}_0^{-1}\Delta\mathbf{Q} \tag{30}$$

where $\mathbf{f}_0(\xi)$ = section flexibility matrix; F_0 = element flexibility matrix; $\mathbf{b}(\xi)$ = equilibrium integrals; and $\Delta\mathbf{Q}$ = element nodal deformations. With reference to the simply supported beam isostatic scheme of Fig. 5, the equilibrium integrals read as follows:

$$\Delta\mathbf{p}(\xi) = \mathbf{b}(\xi)\Delta\mathbf{P} = \begin{bmatrix} 1 & 0 & 0 \\ 0 & 1-\xi & -\xi \\ 0 & 1/l & 1/l \end{bmatrix} \begin{bmatrix} \Delta N \\ \delta M_i \\ \Delta M_j \end{bmatrix} \tag{31}$$

A number of different procedures based on (30) have been used by various authors (Mahasuverachi and Powell 1982; Zeris and Mahin 1988). These so-called ''variable shape functions'' [(30)] are generally more accurate than any other predefined shape functions, although, for a finite-load step, residuals do arise in the sense that equilibrium along the beam is not punctually satisfied. Finding an efficient correction of these residuals has been the major obstacle toward the successful implementation of these equilibrium-based approaches. In Kaba and Mahin (1984), only multilinear constitutive relations were used, and an event-to-event solution strategy proposed (in between the events, the response is linear and the residuals are null). This strategy is still widely used, although it is computationally cumbersome (Powell et al. 1994). A procedure similar to the one described in the following is presented by Spacone et al. (1996).

Once the section forces $\mathbf{p}(\xi)$ that are associated with the section deformation found with (30) are known, the corresponding element forces can be calculated using the virtual work principle in a standard fashion as follows:

$$\Delta\mathbf{P}_0 = \int_{\mathcal{B}} \mathbf{a}^T(\xi)\Delta\mathbf{p}_0(\xi)\, d\xi = \mathbf{F}_0^{-1} \int_{\mathcal{B}} \mathbf{b}^T(\xi)\mathbf{f}_0(\xi)\Delta\mathbf{p}_0(\xi)\, d\xi \tag{32}$$

The residuals, which are calculated as the difference between the section forces associated via the constitutive behavior to the section deformations [(30)] and the stress resultants in equilibrium with the element nodal forces [(31)], as shown in Fig. 6, can be written as

$$\mathbf{r}_{p,0}(\xi) = \Delta\mathbf{p}[\Delta\mathbf{q}_0(\xi)] - \mathbf{b}(\xi)\Delta\mathbf{P}_0 \tag{33}$$

A corrective strain field $\Delta\mathbf{q}_h(\xi)$ can be calculated from these section residuals using the section flexibility matrix as follows (Fig. 6):

$$\Delta\mathbf{q}_h(\xi) = \mathbf{f}_0(\xi)\mathbf{r}_{p,0}(\xi) = \mathbf{f}_0(\xi)\{\mathbf{b}(\xi)\Delta\mathbf{P}_0 - \Delta\mathbf{p}[\Delta\mathbf{q}_0(\xi)]\} \tag{34}$$

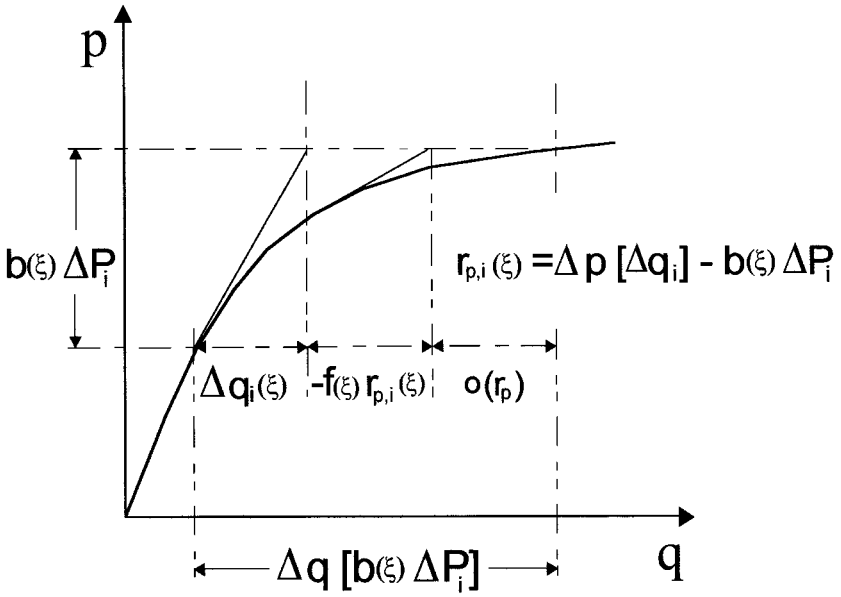

FIG. 6. Section Constitutive Behavior

Notice that while the strain field found with (30) does satisfy the assigned kinematic boundary conditions (element deformations), the strain field found with (34) is homogeneous, in the sense that it vanishes on the boundaries. This is a remarkable property because it allows writing the exact strain field of the nonlinear beam as the sum of a particular term satisfying the boundary condition (30) plus a sum of homogeneous corrective functions found with (34)

$$\Delta\mathbf{q}(\xi) = \mathbf{a}(\xi)\Delta\mathbf{Q} + \sum_{i=1}^{n} \Delta\mathbf{q}_h^i(\xi) \tag{35}$$

The above sequence, i.e., using the strain fields (30) and (34), has proved to be very robust and particularly fast in converging to the (numerically) exact solution. By using the residuals found at iteration step $i - 1$ to calculate a new estimate of the element forces $\Delta\mathbf{P}_i$ and element strain field $\Delta\mathbf{q}_i(\xi)$ at step i, an iterative procedure is obtained, which, in compact notation, can be written as follows:

$$\Delta\mathbf{P}_{i-1} = \mathbf{F}_{i-1}^{-1} \int_{\mathcal{B}} \mathbf{b}^T(\xi)\mathbf{f}_{i-1}(\xi)\Delta\mathbf{p}[\Delta\mathbf{q}_{i-1}(\xi)]\, d\xi \tag{36a}$$

$$\Delta\mathbf{q}_i(\xi) = \Delta\mathbf{q}_{i-1}(\xi) + \mathbf{f}_{i-1}(\xi)\{\mathbf{b}(\xi)\Delta\mathbf{P}_{i-1} - \Delta\mathbf{p}[\Delta\mathbf{q}_{i-1}(\xi)]\} \tag{36b}$$

The procedure that stems out of the above equations is the following:

- The section forces corresponding to the strain field given by (30) are calculated at the integration points along the element $\Delta\mathbf{p}(\xi) = \Delta\mathbf{p}[\Delta\mathbf{q}(\xi)]$.
- The integral in (36*a*) is computed using, for example, the Gauss's quadrature scheme, and the element nodal forces are found.
- A new approximation for the element strain field is found at each integration point, according to (36*b*).
- If a selected norm of (33) or the associated energy $\varepsilon_p = \int_{\mathcal{B}} \mathbf{r}_p^T(\xi)\mathbf{f}(\xi)\mathbf{r}_p(\xi)\, d\xi$ is not less then a specified tolerance, the cycle is repeated.

This procedure has been successfully implemented in all of the previous fiber beam elements developed by the writers (Petrangeli 1996), as it provides significant advantages (Petrangeli and Ciampi 1997) with respect to other solution strategies. Eqs. (36) are particularly suited for the fiber approach because they provide the exact solution with only a few global iterations (satisfaction of equilibrium and local constitutive behavior) of the nonlinear beam problem with assigned end displacement.

SUMMARY

The fiber beam model and the equilibrium-based element solution strategies developed by the writers in the last decade are extended to incorporate the shear modeling at the fiber level. The new model, still retaining many features in common with the traditional fiber element, presents a completely different description of the local constitutive behavior for concrete, using a state-of-the-art macromodel developed for fracture mechanics applications.

The fiber strain vector is found from the section deformation variables ε_0, ϕ, and γ_{xy}, using the classical plane section hypothesis and an additional shape function for the shear strain ϵ_{xy} along the height of the section. The lateral deformations ϵ_y are found instead enforcing equilibrium between the concrete fibers and the transverse reinforcement.

Although much more complicated than the classical fiber model without shear flexibility and still retaining the basic limitations that are intrinsic to the beam theory, the proposed model appears to be capable of modeling the principal mechanisms of shear deformation and failure. It is also believed to represent a substantial step forward with respect to the current models based on truss and strut and tie analogies, which, apart from their grossly idealized mechanics, cannot account, on physical bases, for the interaction between axial, flexural, and shear responses.

The model, as confirmed in the companion paper (Petrangeli 1999), is capable of a good description of a broad range of existing test data, still keeping the input data and computational demand within acceptable limits.

APPENDIX. REFERENCES

Bažant, Z. P., and Bhat, P. D. (1977). ''Prediction of hysteresis of reinforced concrete members.'' *J. Struct. Div.*, ASCE, 103(1), 153–166.

Bažant, Z. P., and Oh, B. H. (1985). ''Microplane model for progressive fracture of concrete and rock.'' *J. Engrg. Mech.*, ASCE, 111(4), 559–582.

Bažant, Z. P., and Ožbolt, J. (1990). ''Nonlocal microplane model for fracture, damage, and size effect in concrete structures.'' *J. Engrg. Mech.*, ASCE, 116(11), 2484–2504.

Bažant, Z. P., and Prat, P. C. (1988). ''Microplane model for brittle-plastic material. Parts I and II.'' *J. Engrg. Mech.*, ASCE, 114(10), 1672–1702.

Bažant, Z. P., Xiang, Y., and Prat, P. C. (1996). ''Microplane model for concrete. I: Stress-strain boundaries and finite strain.'' *J. Engrg. Mech.*, ASCE, 122(3), 245–254.
''Building code requirements for reinforced concrete and commentary.'' (1995). *ACI 318-95*, American Concrete Institute, Detroit, Mich.
Garstka, B., Krätzig, W. B., and Stangenberg, F. (1993). ''Damage assessment in cyclically loaded reinforced concrete members.'' *Structural Dynamics, EURODYN' 93*, Moan ed., Vol. 1, Balkema, Rotterdam, The Netherlands, 121–128.
Guedes, J., and Pinto, A. V. (1997). ''A numerical model for shear-dominated bridge piers.'' *Proc., 2nd Italy-Japan Workshop on Seismic Des. and Retrofit of Bridges*.
Kaba, S. A., and Mahin, S. A. (1984). ''Refined modelling of reinforced concrete columns for seismic analysis.'' *Rep. No. UCB/EERC-84/03*, University of California, Berkely, Calif.
Mahasuverachi, M., and Powell, G. H. (1982). ''Inelastic analysis of piping and tubular structures.'' *Rep. No. UCB/EERC-82/27*, University of California, Berkely, Calif.
Mander, J. B., Priestley, J. N., and Park, R. (1988). ''Theoretical stress-strain model for confined concrete.'' *J. Struct. Engrg.*, ASCE, 114(8), 1804–1826.
Mari, A. R. (1984). ''Nonlinear geometric, material and time dependent analysis of three dimensional reinforced and prestressed concrete frames.'' *Rep. No. UCB/SESM-84/12*, University of California, Berkely, Calif.
Ožbolt, J. (1996). ''Microplane model for quasibrittle materials—Part I theory.'' *Rep. No. 96-1a/AF*, Institut für Werkstoffe im Bauwesen, Stuttgart University, Germany.
Ožbolt, J., and Bažant, Z. P. (1992). ''Microplane model for cyclic triaxial behavior of concrete.'' *J. Engrg. Mech.*, ASCE, 118(7), 1365–1386.
Petrangeli, M. (1991). ''Un elemento finito di trave non-lineare per strutture in cemento armato,'' Msc thesis, University of Rome ''La Sapienza,'' Rome (in Italian).
Petrangeli, M. (1996). ''Modelli numerici per Strutture monodimensionali in cemento armato,'' PhD dissertation, University of Rome ''La Sapienza,'' Rome (in Italian).
Petrangeli, M. (1999). ''Fiber element for cyclic bending and shear of RC structures. II. Verification.'' *J. Engrg. Mech.*, ASCE, 125(9), 1002–1009.
Petrangeli, M., and Ciampi, V. (1997). ''Equilibrium based numerical solutions for the nonliner beam problem.'' *Int. J. Numer. Methods in Engrg.*, 40(3), 423–438.
Petrangeli, M., and Ožbolt, J. (1996). ''Smeared crack approaches—Material modelling.'' *J. Engrg. Mech.*, ASCE, 122(6), 545–554.
Petrangeli, M., Ožbolt, J., Okelo, R., and Eligehausen, R. (1993). ''Mixed method in material modeling of quasibrittle material.'' *Internal Rep. No. 4/18-93/8*, Institut für Werkstoffe im Bauwesen, Stuttgart University, Germany.
Petrangeli, M., and Pinto, P. E. (1994). ''Seismic design and retrofitting of reinforced concrete bridges.'' *Proc., 2nd Int. Workshop on Seismic Des. and Retrofitting of R.C. Bridges*, R. Park, ed., University of Canterbury, New Zealand, 579–596.
Petrangeli, M., Pinto, P. E., and Ciampi, V. (1995). ''Towards a formulation of a fiber model for elements under cyclic bending and shear.'' *Proc., 5th SEDEC Conf. on European Seismic Des. Practice—Res. and Application*, 411–419.
Powell, G. H., Campbell, S., and Prakash, V. (1994). ''DRAIN-3DX base program description and user guide. Version 1.10.'' *Rep. No. UCB/SEMM-94/08*, University of California, Berkeley, Calif.
Ranzo, G., and Petrangeli, M. (1998). ''A finite beam element with section shear modelling for seismic analysis of RC structure.'' *J. Earthquake Engrg.*, 2(3), 443–473.
''R.C. elements under cyclic loading.'' (1996a). *CEB Bulletin 230*, Thomas Telford, London.
''R.C. frames under earthquake loading.'' (1996b). *CEB Bulletin 231*, Thomas Telford, London.
Simo, J. C., and Rifai, M. S. (1990). ''A class of mixed assumed strain method and the method of incompatible modes.'' *Int. J. Numer. Methods in Engrg.*, 29(8), 1595–1638.
Spacone, E., Ciampi, V., and Filippou, F. (1996). ''Mixed formulation of nonlinear beam finite element.'' *Comp. and Struct.*, 58(1), 71–83.
Vecchio, F. J., and Collins, M. P. (1987). ''The modified compression-field theory for reinforced concrete elements subjected to shear.'' *ACI Struct. J.*, 219–231.
Vecchio, F. J., and Collins, M. P. (1988). ''Predicting the response of reinforced concrete beams subjected to shear using modified compression field theory.'' *ACI Struct. J.*, 258–268.
Zeris, C. A., and Mahin, S. A. (1988). ''Analysis of reinforced concrete beam-columns under uniaxial excitation.'' *J. Struct. Engrg.*, ASCE, 114(4).